JCI insight

Atypical response to bacterial co-infection and persistent neutrophilic broncho-alveolar inflammation distinguish critical COVID-19 from influenza

Seppe Cambier, … , Jennifer Vandooren, Paul Proost

JCI Insight. 2021. https://doi.org/10.1172/jci.insight.155055.

Research In-Press Preview COVID-19 Immunology

Graphical abstract

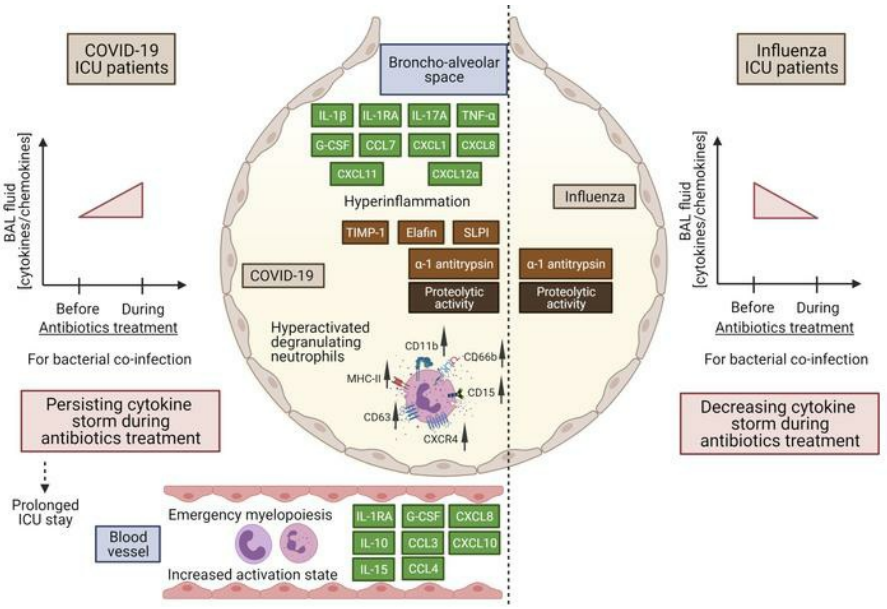

Find the latest version:

https://jci.me/155055/pdf

Atypical response to bacterial co-infection and persistent neutrophilic broncho-alveolar inflammation distinguish critical COVID-19 from influenza

Seppe Cambier[1], Mieke Metzemaekers[1], Ana Carolina de Carvalho[1,2,3], Amber Nooyens[1], Cato Jacobs[4], Lore Vanderbeke[5], Bert Malengier-Devlies[6], Mieke Gouwy[1], Elisabeth Heylen[7], Philippe Meersseman[4], Greet Hermans[8], Els Wauters[9,10], Alexander Wilmer[4], the CONTAGIOUS Consortium, Dominique Schols[7], Patrick Matthys[6], Ghislain Opdenakker[6], Rafael Elias Marques[2], Joost Wauters[4,†], Jennifer Vandooren[6,†] & Paul Proost[1,†,*]

Affiliations:

[1]Laboratory of Molecular Immunology, Department of Microbiology, Immunology and Transplantation, Rega Institute, KU Leuven; Leuven, Belgium.

[2]Brazilian Biosciences National Laboratory – LNBio, Brazilian Center for Research in Energy and Materials – CNPEM; Campinas, Brazil.

[3]Department of Genetics, Microbiology and Immunology, Institute of Biology, University of Campinas (UNICAMP); Campinas, Brazil.

[4]Laboratory for Clinical Infectious and Inflammatory Disorders, Department of Microbiology, Immunology and Transplantation, KU Leuven; Leuven, Belgium.

[5]Laboratory of Clinical Bacteriology and Mycology, Department of Microbiology, Immunology and Transplantation, KU Leuven; Leuven, Belgium.

[6]Laboratory of Immunobiology, Department of Microbiology, Immunology and Transplantation, Rega Institute, KU Leuven; Leuven, Belgium.

[7]Laboratory of Virology and Chemotherapy, Department of Microbiology, Immunology and Transplantation, Rega Institute, KU Leuven; Leuven, Belgium.

[8]Laboratory of Intensive Care Medicine, Department of Cellular and Molecular Medicine, KU Leuven; Leuven, Belgium.

[9]Laboratory of Respiratory Diseases and Thoracic Surgery (BREATHE), Department of Chronic Diseases and Metabolism, KU Leuven; Leuven, Belgium.

[10]Department of Pneumology, University Hospitals Leuven; Leuven, Belgium.

†These authors contributed equally to this work

*Corresponding author: Paul Proost

Email: paul.proost@kuleuven.be

Address: Rega - Herestraat 49 - box 1042 - 3000 Leuven - Belgium

Telephone number: +32 16 32 24 71

Conflict-of-interest:

The authors have declared that no conflict of interest exists.

ABSTRACT

Neutrophils are recognized as important circulating effector cells in the pathophysiology of severe coronavirus disease 2019 (COVID-19). However, their role within the inflamed lungs is incompletely understood. Here, we collected broncho-alveolar lavage (BAL) fluids and parallel blood samples of critically ill COVID-19 patients requiring invasive mechanical ventilation and compared BAL fluid parameters with those of mechanically ventilated influenza patients, as a non-COVID-19 viral pneumonia cohort. Compared to influenza, BAL fluids of COVID-19 patients contained increased numbers of hyperactivated degranulating neutrophils and elevated concentrations of the cytokines IL-1β, IL-1RA, IL-17A, TNF-α and G-CSF, the chemokines CCL7, CXCL1, CXCL8, CXCL11 and CXCL12α, and the protease inhibitors elafin, secretory leukocyte protease inhibitor (SLPI) and tissue inhibitor of metalloproteinases 1 (TIMP-1). In contrast, α-1 antitrypsin levels and net proteolytic activity were comparable in COVID-19 and influenza BAL fluids. During antibiotics treatment for bacterial co-infections, increased BAL fluid levels of several activating and chemotactic factors for monocytes, lymphocytes and NK cells were detected in COVID-19 patients whereas concentrations tended to decrease in influenza patients, highlighting the persistent immunological response to co-infections in COVID-19. Finally, the high proteolytic activity in COVID-19 lungs suggests considering protease inhibitors as a treatment option.

INTRODUCTION

Severe acute respiratory syndrome coronavirus 2 (SARS-CoV-2) infection and the resulting coronavirus disease 2019 (COVID-19) continue to pose a major threat to global health and economy, with >245 million confirmed cases and >5 million deaths up to November 2021 (WHO, covid19.who.int). COVID-19 is heterogeneous in its severity with most patients being asymptomatic or facing mild symptoms. However, up to 20% of patients develop severe acute respiratory distress syndrome (ARDS) thus requiring intensive care (1). The systemic hyperinflammatory response in severe COVID-19 is associated with dysregulation of the immune system and is characterized by an atypical cytokine storm, lymphopenia and increased neutrophil counts in blood (2-4). Neutrophils, as the most abundant circulating leukocytes in humans, are among the first responders to infection exploiting a multitude of oxidative and non-oxidative effector mechanisms (5, 6). In the blood of patients with severe COVID-19, the presence of immature neutrophils has been evidenced, indicating a situation of emergency myelopoiesis (7-9). Besides, a state of increased neutrophil activation in the circulation, together with elevated levels of neutrophil-mobilizing/activating factors, neutrophil-derived proteases, and neutrophil extracellular traps (NETs) associated with immunothrombosis, was observed in critically ill patients (7, 10-13). Moreover, myeloid-derived suppressor cell-like neutrophils with an immunosuppressive effect on T-cells were seen (8, 14, 15). Thus, growing consensus exists that neutrophils are key effector cells in severe COVID-19. Therefore, a better understanding of the role of neutrophils that have infiltrated the lungs is required. Within the broncho-alveolar space, increased neutrophil counts with a heterogeneous phenotype are seen, but most information is available from single-cell transcriptomics studies whereas information on protein levels is limited (16-18). Moreover, the effect on the inflammatory response of bacterial or fungal co-infection(s)

in mechanically ventilated COVID-19 patients requires further investigation. Indeed, ventilator-associated lower respiratory tract infections are significantly more prevalent in COVID-19 compared to influenza patients or ventilated patients without viral infections (19) and are associated with a longer duration of ventilation, hospitalization at intensive care units (ICU) and mortality (20, 21).

Here, we collected blood and broncho-alveolar lavage (BAL) fluid samples from critically ill COVID-19 patients, hospitalized in ICU and requiring invasive mechanical ventilation or extracorporeal membrane oxygenation (ECMO). The aim was to phenotypically characterize neutrophils, determine cytokine/chemokine levels, define the protease-protease inhibitor balances within the lungs and to study the effect of co-infections in this context. The obtained results were compared with those of blood samples from healthy volunteers and with BAL samples from critically ill influenza patients in the ICU, as a non-COVID-19 viral pneumonia control group.

RESULTS

Patient cohort

Seventeen COVID-19 and 14 critically ill influenza patients were recruited at the ICU of the University Hospital Leuven (Figure 1, A and B; Table 1). COVID-19 patients had a comparable 'Acute Physiology And Chronic Health Evaluation II' (APACHE II) score at ICU admission but stayed for a significantly longer period of time in the ICU compared to influenza patients (Figure 1, C and D). All COVID-19 patients and the vast majority of influenza patients had invasive mechanical ventilation as minimum level of respiratory support with no significant differences in the 'Sequential Organ Failure Assessment' (SOFA) scores of the COVID-19 compared to the influenza patients at the moment of BAL and blood sampling (Figure 1E). Blood neutrophil counts and the proportion of neutrophils (as a percentage of total leukocytes) in the BAL fluid were not significantly different between COVID-19 and influenza patients (Figure 1, F and G). However, the absolute neutrophil count in the BAL fluid was significantly increased in COVID-19 compared to influenza patients (Figure 1H). Table 1 contains detailed characteristics of patients included in this study.

Hyperactivated neutrophils expressing novel surface proteins in BAL fluid from COVID-19 patients

BAL and peripheral blood neutrophils were phenotypically characterized with a focus on the expression of adhesion molecules, activation/maturation markers, Fcγ receptors and chemoattractant receptors using multicolor flow cytometry (Figure 2 and 3; Supplemental Figure 1). We confirmed the presence of immature ($CD10^-$) neutrophils in the circulation of COVID-19 patients (Figure 2A), indicating emergency myelopoiesis, as we have demonstrated before (7). BAL fluids contained significantly more mature neutrophils (> 90% $CD10^+$ neutrophils) in

comparison with parallel blood samples. Previously, an increased neutrophil activation state was seen in the blood of COVID-19 ICU patients (7). In comparison to blood neutrophils of healthy controls, we confirmed this increased activation state in critically ill COVID-19 patients, as shown by e.g. significantly decreased expression of L-selectin (CD62L) (Figure 2B; Supplemental Figure 1A). However, BAL fluid neutrophils showed significantly more pronounced signs of activation than neutrophils in the circulation. They almost completely lacked L-selectin expression and were characterized by increased levels of the integrins α_M (CD11b) and α_X (CD11c) in comparison to matched blood neutrophils (Figure 2, B-D; Supplemental Figure 1A). Also, a minor but significant percentage of the BAL fluid neutrophils had upregulated the α_4 integrin CD49d (Figure 2E), which plays a role in neutrophil recruitment during bacterial lung infection in mice (22) and is upregulated by aged neutrophils (23). Moreover, in comparison to blood neutrophils, BAL neutrophils had increased expression of CD66b, Sialyl-Lewis^X (i.e. the selectin ligand CD15) and the tetraspanin CD63 (Figure 2, F-H; Supplemental Figure 1B), markers that can be upregulated rapidly on the neutrophil membrane by means of degranulation (24). For complement receptor 1 (CD35), no significant differences were seen between the study groups (Figure 2I). The activation marker CD69, which is absent on quiescent neutrophils, was also detected on a significantly increased proportion of the BAL neutrophils (Figure 2J). Finally, moderate expression of the antigen-presenting MHC class II molecules HLA-DR and HLA-DQ was detected on BAL fluid neutrophils (Figure 2, K and L). The latter indicates that part of the BAL fluid neutrophils might possibly acquire antigen-presenting capacities.

Although most blood neutrophils stained positive for CXCR1 and CXCR2, the relative expression levels of these chemoattractant receptors were significantly lower on blood neutrophils from

COVID-19 patients compared to blood neutrophils from healthy controls (Figure 3, A and B; Supplemental Figure 1, C and D). BAL fluid neutrophils displayed even lower levels of CXCR1 and CXCR2 as compared to blood cells (Figure 3, A and B), and a significant proportion of the BAL neutrophils completely lacked CXCR1 and CXCR2 (Supplemental Figure 1, C and D). In addition, some neutrophils in the BAL fluid had upregulated CXCR4, a chemokine receptor characteristic for immature or aged neutrophils (25, 26), with some patients having up to 40% $CXCR4^+$ neutrophils (Figure 3C). To discriminate between these two subsets, we defined aged neutrophils as $CXCR4^+CD49d^+CD10^+$ and immature neutrophils as $CXCR4^+CD49d^-CD10^-$ and found both subsets present in the BAL samples (Supplemental Figure 1E). Among the other prototypical chemoattractant receptors present on neutrophils, the expression of complement receptor C5aR was significantly decreased (Figure 3D; Supplemental Figure 1F) whereas the formyl peptide receptors FPR1 and FPR2 were significantly increased on COVID-19 BAL fluid neutrophils (Figure 3, E and F; Supplemental Figure 1G), in comparison to blood neutrophils. A small population of BAL fluid neutrophils (0-20%) also expressed CCR1 or CCR2, two chemokine receptors that are not typically expressed on neutrophils (Figure 3, G and H). Besides, a significantly upregulated expression of CD14 (the co-receptor for lipopolysaccharide binding to Toll-like receptor 4) was seen (Figure 3I). Finally, expression of the low-affinity Fcγ receptor III (CD16) was significantly decreased whereas expression levels of Fcγ receptor II (CD32) and Fcγ receptor I (CD64) were significantly increased on neutrophils in BAL fluid compared to blood neutrophils of COVID-19 patients (Figure 3, J-L; Supplemental Figure 1, H and I). No significant differences were detected in the expression of IL1-R2 and the chemoattractant receptor BLTR1 (Supplemental Figure 1, J and K) and no expression of IL-1R1, ICAM-1 or CXCR3 was detected. In conclusion, we show with multiple parameters that neutrophils from critically ill COVID-19

patients are partially immature, activated cells in the circulation, whereas those that have migrated to the lungs are mostly mature, hyperactivated and acquire a novel repertoire of surface proteins.

Elevated cytokine and chemokine levels in BAL fluid from COVID-19 compared to influenza patients

To determine the broncho-alveolar inflammation at the protein level, cytokine and chemokine levels were quantified in BAL fluids from COVID-19 and influenza patients, and in plasma from COVID-19 patients and healthy controls by multiplex assays (Figure 4 and 5). Plasma levels of interleukin-1 receptor antagonist (IL-1RA), IL-10, IL-15, G-CSF, and of the chemokines CCL3, CCL4, CXCL8 and CXCL10 were significantly increased in COVID-19 patients compared to those of healthy controls. No significant differences between COVID-19 patients and healthy donors were detected for IFN-γ, TNF-α, granzyme B, IL-6, IL-12/IL-23p40, IL-18, IL-23, CCL2, CCL7, CCL8, CXCL1, CXCL11 and CXCL12α. Circulating GM-CSF, IL-1β, IL-4, IL-5, IL-12p70 and IL-17A concentrations were below the detection limit for most donors.

In the BAL fluid of COVID-19 patients, significantly increased and extremely high levels of the cytokines IL-1β, IL-1RA, IL-17A, TNF-α and G-CSF, and the chemokines CCL7, CXCL1, CXCL8, CXCL11 and CXCL12α were found in comparison to BAL fluid of influenza patients. IFN-γ, granzyme B, IL-6, IL-10, IL-15, IL-18, CCL2, CCL3, CCL4, CCL8, CXCL5 and CXCL10 levels were not significantly different from levels in BAL fluid of influenza patients, although a tendency towards increased concentrations was seen in the COVID-19 patients. GM-CSF, IL-4, IL-5, IL-12p70, IL-12/IL-23p40, IL-23 and CCL11 were below the detection limit for most donors. Remarkable is the large variation seen amongst the different COVID-19 BAL samples. A positive correlation was found between COVID-19 BAL fluid levels of IL-15 and CXCL10 or CCL2;

cytokines/chemokines involved in monocyte, lymphocyte, and NK cell functions (Figure 5, M and N). Moreover, a positive correlation was seen between levels of IL-1β or IL-17A and CXCL8 in the BAL fluid of the COVID-19 patients (Figure 5, O and P). To conclude, the COVID-19 hypercytokinemia was associated with significantly elevated levels of cytokines and chemokines in the BAL fluid compared to the BAL fluid of influenza ARDS patients.

Increased levels of protease inhibitors and similar net proteolytic activity in BAL fluid from COVID-19 compared to influenza patients

Neutrophils store different proteases inside their granules and these are released upon activation. However, a balance with protease inhibitors is crucial to prevent collateral damage to healthy (lung) tissues. Significantly increased levels of the metalloproteinase inhibitor tissue inhibitor of metalloproteinases 1 (TIMP-1) and of TIMP-1 in complex with MMP-9 were found in COVID-19 BAL fluids compared to influenza BAL fluids (Figure 6, A and B). Moreover, highly elevated levels of the locally produced serine protease inhibitors secretory leukocyte protease inhibitor (SLPI) and elafin were found in the BAL fluid of COVID-19 in comparison to influenza patients (Figure 6, C and D). In contrast, comparable levels of a major circulating serine protease inhibitor, α-1 antitrypsin (serpin A1), were detected in the BAL fluid of COVID-19 versus influenza patients (Figure 6E).

Due to the complex interactions between proteases and protease inhibitors, we measured the net proteolytic activity within the lungs. No significant differences in gelatinolytic activity or total MMP activity were found in the BAL fluid of COVID-19 versus influenza patients (Figure 6, F and G). However, a remarkably large variation was seen amongst the different patient samples. As we did not detect gelatinolytic activity within the parallel plasma samples (due to collection in tubes coated with EDTA), we applied the same analysis procedure on plasma samples (collected

with tubes coated with citrate) from COVID-19 patients in the ICU included in our previous study to allow for comparison (7). For all these plasma samples, the relative activity is maximally equivalent to 39.3 pM MMP-9. For many samples activities fell below the detection limit (estimated to be equivalent to 4.88 pM MMP-9) (Supplemental Figure 2, A and B). In some patient BAL samples, gelatinolytic activity was also below the detection limit, whereas other samples exhibited up to 50-fold higher activities (Figure 6F; Supplemental Figure 2, A and B). Comparable variability was observed for elastinolytic activity in the BAL fluids. A trend for a 5-fold increase in median elastinolytic activity was seen in the BAL fluids of COVID-19 compared to influenza patients, but data did not reach significance (Figure 6H). By introducing protease inhibitors in the enzyme activity assays, we were able to assign the gelatinolytic and elastinolytic activities to both MMPs and serine proteases (Supplemental Figure 2, C-F). One of the major neutrophil proteases contributing to the degradation of elastin is the serine protease neutrophil elastase (27). However, no significant differences in neutrophil elastase concentrations were found between COVID-19 and influenza BAL fluids (Figure 6I). Interestingly, levels of IL-1β and CXCL8 in COVID-19 BAL fluid correlated positively with the elastinolytic and gelatinolytic activities measured (Figure 6, J and K; Supplemental Figure 2, G and H). Finally, we uncovered a moderate but significant negative correlation between α-1 antitrypsin levels and gelatinolytic activity in the BAL fluid from COVID-19 patients, with higher concentrations of α-1 antitrypsin preventing severe proteolytic activity (Figure 6L). In conclusion, although high levels of metalloproteinase and serine protease inhibitors were detected in the BAL fluid of COVID-19 patients, the net proteolytic activity was not significantly altered compared to influenza patients.

High cytokine/chemokine levels persist in BAL fluid from COVID-19 patients during antibiotics treatment for a bacterial co-infection

Bacterial and fungal co-infections are common in COVID-19 ICU patients and are associated with a longer duration of ventilation (19, 20). Therefore, it was interesting to study the effect of co-infections on the inflammatory response. COVID-19 and influenza patient BAL samples were categorized based on the presence or absence of (a) co-infection(s) and the type and timing of the co-infection(s). Co-infections were mostly of bacterial or combined bacterial-fungal origin (only one patient was diagnosed with a fungal co-infection only) in COVID-19 patients, whereas in influenza patients all co-infections were bacterial with only one bacterial-fungal co-infection diagnosed (Figure 1, A and B). No significant differences were found in cytokine/chemokine levels (Supplemental Figure 3 and Supplemental Figure 4), protease activity and levels of proteases and protease inhibitors (Supplemental Figure 5) in the BAL fluid of COVID-19 patients with or without bacterial or combined bacterial-fungal co-infections. BAL fluid levels of TIMP-1/MMP-9 complexes were significantly elevated in COVID-19 patients having a bacterial-fungal co-infection compared to COVID-19 patients having a bacterial co-infection. However, for these interim analyses, samples were stratified solely based on the presence of a co-infection and the type of co-infection, without considering the timing of the co-infection. Therefore, we further subdivided the bacterial co-infections in acute (early phase of co-infection with clinical/biochemical worsening and antibiotics not yet or recently started), midphase (signs of improvement with ongoing antibiotic therapy) or late phase (final days of antibiotic therapy nearing complete remission) based on the timing of the BAL sample analyzed relative to the co-infection time course (Figure 7). Concentrations of IL-15, granzyme B, CCL2, CCL7, CCL8, CXCL1, CXCL10, CXCL11 and CXCL12α, i.e. inflammatory mediators associated with attraction or activation of monocytes, lymphocytes and NK cells, were significantly increased in the BAL fluid of COVID-19 patients in the mid- or late phase compared to patients in the acute

phase of the co-infection (Figure 7, A-I). IL-15, CCL8 and CXCL10 levels were also significantly elevated in the BAL fluid of COVID-19 patients in the mid- or late phase of a co-infection compared to patients without co-infections. Thus, despite treatment with antibiotics, the highest BAL fluid concentrations of these cytokines/chemokines in COVID-19 patients were detected in later phases of the bacterial co-infection. This contrasts with the influenza BAL samples, for which these cytokine/chemokine levels tended to be lower in later phases of a bacterial co-infection compared to the acute phase. Neutrophil counts in the BAL fluid of COVID-19 patients having an acute co-infection were significantly increased compared to COVID-19 patients without co-infection. Furthermore, neutrophil counts did not become lower upon treatment with antibiotics, in contrast with influenza patients in whom a trend for reduction was seen (Figure 7J). In addition, significantly increased BAL fluid levels of the protease inhibitors SLPI and elafin were found during the mid/late phase compared to the acute phase of the co-infection in COVID-19 patients (but not in influenza patients) (Figure 7, K and L). However, in COVID-19 patients, this did not correlate to significant changes in proteolytic activity or other protease/protease inhibitor levels during different phases of the co-infection (Supplemental Figure 6). In addition, levels of the other cytokines, mononuclear leukocyte-derived CCL3 and CCL4 and the neutrophil attractant chemokines CXCL5 and CXCL8 were not significantly different during different phases of the co-infection (Supplemental Figure 7 and Supplemental Figure 8, A-D). No significant differences were noticed in the timing (days after ICU admission) of the BAL sampling (Supplemental Figure 8E) or the SARS-CoV-2 and influenza viral load (Supplemental Figure 8F) in the BAL samples from COVID-19 and influenza patients without co-infection, or patients in the acute or mid/late phase of a bacterial co-infection. Moreover, no correlations were found between the cytokine/chemokine levels and the viral load in the BAL samples, excluding an exclusively viral

effect on the elevated inflammatory mediators during the later phases of the bacterial co-infection. In conclusion, despite antibiotics treatment for bacterial co-infections, critically ill COVID-19 patients kept very high levels of IL-15, granzyme B, CCL2, CCL7, CCL8, CXCL1, CXCL10, CXCL11, CXCL12α and the serine protease inhibitors SLPI and elafin in their lungs, whereas after influenza infection these molecules rather returned to basal levels in the recovery phases. This suggests that bacterial co-infection triggers a stronger and more long-lasting inflammatory response in COVID-19 patients, even during treatment with antibiotics and corticosteroids.

DISCUSSION

It is now well established that an atypical cytokine storm drives the systemic inflammation in severe COVID-19 (2, 3, 11, 28, 29), which is confirmed by our results. In the BAL fluid of COVID-19 compared to critically ill influenza patients, we detected elevated and extremely high levels of the cytokines IL-1β, IL-1RA, IL-17A, TNF-α and G-CSF, and the chemokines CCL7, CXCL1, CXCL8, CXCL11 and CXCL12α, expanding earlier reports showing increased concentrations of inflammatory mediators compared to BAL fluid of healthy donors or patients with moderate influenza or COVID-19 (29-31). Single-cell transcriptomics and flow cytometry studies on the BAL fluid of COVID-19 patients showed elevated numbers of pro-inflammatory monocyte-derived macrophages in severe cases compared to cases that were rather moderate or non-COVID-19 pneumonia (16, 17, 31-33). These macrophages represent a potentially important source of pro-inflammatory mediators. Considering the discovery of CXCL8 as an IL-1β-induced protein (34), we found that COVID-19 BAL fluid levels of CXCL8 and IL-1β correlated positively with each other and with levels of IL-17A. Clonally expanded tissue-resident memory-like Th17 cells, with expression of *IL17A* in the lungs, and elevated IL-17A levels in the BAL fluid, were detected in patients with severe COVID-19 (35). Evidence for a cross-talk between human neutrophils and Th17 cells was already shown before (36), with additional evidence for neutrophils promoting the induction of Th17 cells in COVID-19 patients (37).

The 10 to 100-fold higher levels of the most potent human neutrophil-attracting chemokine CXCL8 and the neutrophil-attracting chemokines CXCL1 and CXCL5 in the BAL fluid of COVID-19 versus influenza patients, could provide an explanation for the major neutrophil infiltration in the lungs. Lung neutrophils displayed a hyperactivated phenotype, in comparison to

the already activated neutrophils in the blood, as evidenced by near-complete shedding of L-selectin, downregulation of CD16, CXCR1, CXCR2 and C5aR and upregulation of CD11b, CD11c, CD49d, FPR1, FPR2, CD32, CD64, CD69, CD14, CD66b, CD15 and CD63. Moreover, NETs have been previously detected in the airway, interstitial, and vascular compartments of the lungs of COVID-19 patients (38). It has been proposed that a self-sustaining positive feedback loop of systemic and neutrophil intrinsic CXCL8 production could lead to an activated, prothrombotic neutrophil phenotype characterized by degranulation and NET formation (39). Interestingly, a significant portion of the BAL fluid neutrophils expressed CXCR4, a receptor present on immature neutrophils in the bone marrow and shown to reappear on aged neutrophils (26). Expression of *CXCR4* by neutrophils in COVID-19 patients was already shown by single-cell RNA sequencing in the lungs (9). Based on (absence of) co-expression of CD10 and CD49d, it seemed that both immature as well as aged neutrophils are present in the BAL fluid. The immature neutrophils might represent the 'progenitor' neutrophils already found before (17). Finally, some neutrophils upregulated antigen-presenting molecules HLA-DR and HLA-DQ within the BAL fluid. Such neutrophils can actively present antigens to T cells, potentially playing a role in the regulation of adaptive immunity (40). Interestingly, these 'hybrid' neutrophils were previously found in BAL fluid by single-cell RNA sequencing (17).

Upon activation, neutrophils release several proteases, protease inhibitors and anti-microbial proteins into the extracellular environment (6, 41). In ARDS patients, continuous proteolytic damage can cause sustained inflammatory cell infiltration, progressive lung tissue damage, fibrin deposition, hyaline membrane formation and in some cases triggers fibroblast activation and fibrosis (42). Indeed, diffuse alveolar damage (DAD) is a common characteristic seen in *post-*

mortem histopathological lung analysis from patients who died from COVID-19 (43). Elastin (and other extracellular matrix protein)-degrading proteases released by neutrophils could contribute to alveolar damage, resulting in protein-rich alveolar edema (44, 45). Neutrophil elastase, proteinase 3, cathepsin G and activated cathepsin C have been detected in endotracheal aspirates of mechanically ventilated patients with COVID-19 or non-COVID-19-associated ARDS (46). We did not measure significant differences in neutrophil elastase concentrations between COVID-19 and influenza BAL fluid. However, neutrophil elastase concentrations were much higher in comparison to the concentrations we found in COVID-19 plasma samples (7). In addition, we detected 100- to 1000-fold higher levels of SLPI and elafin in the BAL fluid of COVID-19 in comparison to influenza patients. These serine protease inhibitors are produced at mucosal surfaces in the lungs by epithelial cells and leukocytes including neutrophils, and provide a local inducible anti-protease and anti-inflammatory safeguard (47). Despite these high levels of protease inhibitors in COVID-19 patients, the net proteolytic activity in the lungs was not significantly altered compared to influenza patients, indicative for concomitant high protease levels. Follow-up research is required to unveil the putative roles played by proteases other than neutrophil elastase in the pathology of COVID-19 versus influenza. The abundantly present protease inhibitors in the COVID-19 patient lungs could also be inactivated by proteolytic cleavage and still remain detectable by ELISA. For the protease inhibitor SLPI, it has been shown that MMP-9 and other neutrophil-derived proteases can cleave SLPI, resulting in a reduced capacity to inhibit neutrophil elastase activity (48).

The circulating, neutrophil elastase-targeting, acute-phase protein α-1 antitrypsin (serpin A1) was abundantly present in the BAL fluid of both COVID-19 and influenza patients. Neutrophil elastase

can contribute to proteolysis of the SARS-CoV-2 glycoproteins allowing membrane fusion in the host (49). Therefore, by inhibiting neutrophil elastase, α-1 antitrypsin may impair SARS-CoV-2 infection. Besides, α-1 antitrypsin was shown to inhibit transmembrane serine protease 2 (TMPRSS2), the protease priming the SARS-CoV-2 spike protein for entry into host cells (50). We showed a negative correlation between α-1 antitrypsin levels and gelatinolytic activity in the BAL fluid of the COVID-19 patients, with higher concentrations of α-1 antitrypsin preventing severe proteolytic activity. Therefore, for patients having high proteolytic activity within the lungs, the use of inhibitors targeting neutrophil-derived proteases might be a useful additional treatment strategy to prevent excessive proteolytic damage. As IL-1β and CXCL8 levels in the BAL fluid correlated to the proteolytic activity, such high levels could be a relevant indication for treatment. Interestingly, BAL fluid levels of CXCL8 were specifically shown to be predictive for COVID-19 severity and may also serve as potential biomarker for predicting COVID-19 progression (29). Due to both its antiviral and anti-inflammatory role, α-1 antitrypsin was already suggested as a good candidate for treatment of COVID-19 ARDS (51-53). Currently, several clinical trials are ongoing evaluating the use of α-1 antitrypsin and neutrophil-derived protease inhibitors for COVID-19 treatment (NCT04385836, NCT04547140, NCT04495101, NCT04817332; ClinicalTrials.gov). In short, hospitalized COVID-19 patients are being recruited for phase 2 clinical trials for efficacy evaluation of α-1 antitrypsin (either by intravenous injection or inhalation) aiming to reduce mortality or requirement of intensive care. Moreover, a phase 3 clinical trial is investigating the potential of Brensocatib (INS1007) as a novel therapy for adult patients hospitalized with COVID-19. Brensocatib is an oral reversible inhibitor of dipeptidyl peptidase 1 (DPP-1), an enzyme responsible for activation of neutrophil serine proteases.

Interestingly, Brensocatib has been shown to reduce neutrophil serine protease activity and improves clinical outcome in patients with bronchiectasis (54).

The presence of co-infections in the lungs could have an important influence on disease outcomes as it was shown that co-infections are associated with a longer duration of ventilation in critically ill COVID-19 patients (19, 20). It was proposed that the COVID-19 cytokine storm may be the result of synergistic interactions among Toll-like receptors (TLRs) and nucleotide-binding oligomerization domain-like receptors (NLRs) due to combined infections of SARS-CoV-2 and other microbes (55). When stratifying bacterial co-infections based on the timing of the BAL sample analyzed relative to the co-infection time course, we found that BAL fluid levels of several inflammatory proteins acting on monocytes, lymphocytes and NK cells in COVID-19 patients persisted or even increased beyond the acute phase of a co-infection, when patients remained on antibiotic treatment. This contrasts with the (trend for a) drop in release of these mediators in antibiotics-treated ICU influenza patients suffering from co-infections. As viral loads were comparable in the COVID-19 BAL samples taken during the acute or later phases of a bacterial co-infection, we hypothesize that it is this second bacterial stimulus and the synergy between SARS-CoV-2 and bacterial pathogen-associated molecular patterns that prevent the reduction of these inflammatory mediators on the long-term, during antibiotics and corticosteroids, treatment. Together with the diminished type I and type III IFN production (untuned antiviral immunity) in COVID-19 in comparison to influenza (56) and defects in the sensing of viral RNA (inborn errors in type I IFN immunity) in some patients with life-threatening COVID-19 (57), this may at least partially account for the prolonged stay and higher mortality of COVID-19 patients at ICU. Given the many clinical trials investigating the use of cytokine-modulating therapies for COVID-19

treatment, it would be worthwhile to study the influence of these therapies on the inflammatory response to co-infections and the antimicrobial treatment.

This study has some unavoidable limitations. Firstly, since no influenza patients were treated in our university hospital during the COVID-19 pandemic, we could not collect influenza BAL neutrophils for flow cytometric analysis and were restricted to the analysis of influenza BAL fluid collected during the previous winter. Secondly, the number of saline aliquots used during BAL sampling was slightly different between influenza and COVID-19 patients. The amount of fluid recovered from the total volume instilled is also slightly different for every patient. These are well-known limitations of BAL fluid sampling for which it is difficult to correct and might have consequences regarding protein concentrations or activity. However, BAL sampling was always performed on the same location in the lungs and with the same volume of saline per aliquot, ensuring that comparable areas in the lungs are included. Due to the observed specific differences between COVID-19 and influenza patients (for certain parameters up to 1000-fold, other factors are similar), we are confident that the comparisons we have made are reliable. Thirdly, our sample size is limited, which is mainly due to practical limitations that come with the analysis of neutrophils and BAL fluids (use of a biosafety level 3 (BSL3) facility and ethical permission). Fourthly, no time component was included in our analysis. Some cytokine, chemokine and protease inhibitor levels tended to be lower in COVID-19 patient BAL samples collected later during ICU stay compared to samples collected earlier during ICU stay (Supplemental Figure 9). However, for other cytokines and chemokines, this trend was not visible and since the clinical situation of the COVID-19 patients is highly variable during hospital stay, an adequate analysis of data kinetics was difficult. Moreover, the COVID-19 BAL samples collected early during ICU

stay would be most “comparable” to the BAL samples of the influenza patients with respect to BAL sampling timing. The differences between these early COVID-19 and influenza patient samples are even more pronounced for certain biomarkers. Moreover, timing of BAL sample collection did not influence the co-infection data significantly (Supplemental Figure 8E). Finally, there might be other unavoidable factors confounding our analysis: patients had divergent co-morbidities, were on different therapies, received artificial ventilation and had different co-infections.

In conclusion, we show hyper-inflammation characterized by significantly increased cytokine and chemokine levels, hyperactivated neutrophils and elevated levels of protease inhibitors TIMP-1, SLPI and elafin in the lungs of critically ill COVID-19 patients in comparison to influenza patients. In contrast to influenza patients, the cytokine storm in the lungs persisted or even increased during antimicrobial treatment for a bacterial co-infection in COVID-19 patients. This suggests that synergy between bacterial co-infections and SARS-CoV-2 triggers a stronger production of these inflammatory mediators on the long term, despite antibiotics and corticosteroids treatment, which may at least partially account for the prolonged stay at ICU of COVID-19, in comparison to influenza patients.

METHODS

Study design

Seventeen critically ill adult COVID-19 patients were recruited at the University Hospital Leuven between November and December 2020. All patients were on invasive mechanical ventilation or received ECMO in ICU. In total, 31 fresh blood and parallel BAL samples were collected from the COVID-19 patients in a period 4-37 days after ICU admission, upon clinical indication (Figure 1A). Blood samples from age- and sex-matched healthy individuals were investigated for comparative purposes. Measurements were compared to stored BAL supernatant of 14 adult influenza patients with invasive mechanical ventilation as the minimum level of respiratory support (except for 2 samples) collected at 4-6 days after ICU admission in the influenza season of 2019 and 2020 (Figure 1B). The objectives of this study were (1) to characterize the phenotype of BAL fluid and parallel blood neutrophils in critically ill COVID-19 ICU patients and compare this to blood neutrophils of healthy controls; (2) to determine the levels of inflammatory cytokines, chemokines, proteases and protease inhibitors within the plasma and BAL fluid of COVID-19 patients and compare this to influenza patients as a non-COVID-19 viral pneumonia control group; and (3) to study the effect of a bacterial or fungal co-infection(s) in this context.

Assessment of co-infections

Two clinicians (LV and JW) assessed the presence of bacterial and fungal co-infection(s) independently. Biochemical and microbial test culture results were evaluated in combination with clinical and radiological characteristics to detect all clinically relevant co-infections. Bacterial co-infection was scored as acute (early phase of co-infection with clinical/biochemical worsening and antibiotics not yet or recently started), midphase (signs of improvement with ongoing antibiotic therapy) or late phase (final days of antibiotic therapy nearing complete remission) based on the

timing of BAL sample analyzed relative to the co-infection time course. Diagnosis of probable invasive pulmonary aspergillosis was based on radiological abnormalities in combination with clinical signs and mycological evidence (positive galactomannan in BAL and/or serum and/or presence of *Aspergillus fumigatus* in BAL culture) as defined by Koehler et al. (58).

Processing of blood and BAL samples

Fresh blood and BAL samples were processed within 30 minutes of withdrawal. Blood samples were collected in vacutainer tubes (BD Biosciences) treated with EDTA. Blood samples were spun down for 10 minutes at 400 *g*. The supernatant was collected and centrifuged for 20 minutes at 16000 *g* to obtain platelet-free plasma. BAL samples from COVID-19 patients were collected via bronchoscopy by instilling 2 aliquots of 20 mL sterile saline in the right middle lobe or lingula after which the returned fractions were immediately pooled for further processing. BAL samples from influenza patients were collected by instilling 3-5 aliquots of 20 mL sterile saline in the right middle lobe or lingula. BAL samples from COVID-19 patients were processed in the biosafety level 3 (BSL3) facility of the Rega Institute, KU Leuven. BAL samples were centrifuged for 8 minutes at 500 *g* to collect BAL supernatant. Plasma and BAL supernatant were stored until further use at -80°C. To collect cells for flow cytometry, the cell pellet was resuspended 1:1 in 0.1% dithiothreitol (DTT), vortexed for 15 minutes and filtered through a nylon filter (Falcon 40 µm cell strainer, Corning) to remove excess mucus. After centrifugation, the supernatants were discarded, and the pellets were resuspended in DPBS for counting.

Isolation of neutrophils

Blood neutrophils used for phenotypical characterization were isolated from the whole peripheral blood by immuno-magnetic negative selection according to the manufacturer's instructions

(EasySep™ Direct Human Neutrophil Isolation Kit; Stemcell Technologies) within 30 minutes of withdrawal.

Phenotypical analysis of neutrophils

Neutrophil phenotyping was performed on isolated blood neutrophils and the BAL cell pellet (without previous neutrophil purification). Cells were treated with FcR block (Miltenyi Biotec) and Fixable Viability Stain 620 (BD Biosciences) or Zombie Aqua 516 (Biolegend) for 15 minutes at room temperature. Subsequently, cells were washed with flow cytometry buffer [PBS + 2% (*v/v*) FCS + 2 mM EDTA] and stained with fluorescently labeled antibodies. Antibodies used in this study were titrated in-house and are listed in Supplemental Table 1. Following incubation for 25 minutes (on ice), cells were washed with flow cytometry buffer and fixed with BD Cytofix (BD Biosciences). Results were analyzed using a BD LSRFortessa™ X-20 (BD Biosciences) equipped with DIVA software (BD Biosciences). FlowJo software (BD Biosciences) was used for downstream analysis. Neutrophils were gated as $CD16^{+}CD66b^{+}$ cells within the population of living, single cells (Supplemental Figure 10).

Quantification of cytokines, chemokines, proteases, and protease inhibitors

Plasma and BAL supernatant concentrations of IL-1β, IL-1RA, IL-4, IL-5, IL-6, IL-10, IL-12p70, IL-12/IL-23p40, IL-15, IL-17A, IL-18, IL-23, IFN-γ, TNF-α, G-CSF, GM-CSF, granzyme B, CXCL5, CXCL10, CXCL11, CXCL12α, CCL2, CCL3, CCL4, CCL7, CCL8 and CCL11 were measured using customized Meso Scale Discovery multiplex assays. CXCL8 concentrations in BAL were evaluated using a specific sandwich ELISA developed in our laboratory (7). CXCL1, neutrophil elastase, TIMP-1, TIMP-1/MMP-9 complexes, SLPI, Serpin A1 and Trappin-2/Elafin were quantified by DuoSet ELISAs (R&D Systems) in BAL supernatant.

Measurement of elastinolytic, gelatinolytic and MMP activity

To measure gelatinase or metalloproteinase activity, 15 µl of dye-quenched gelatin (DQ™-gelatin; Thermo Fisher Scientific) [final concentration of 5 µg/mL] or OmniMMP substrate peptide (Mca-PLGL-Dpa-AR-NH_2, cat. no. BML-P126-0001, Enzo Life Sciences) [final concentration of 5 µg/mL] in assay buffer (50 mM Tris, 150 mM NaCl, 5 mM $CaCl_2$, 0.01% Tween-20, pH 7.4), was added to 5 µL BAL supernatant, respectively. A standard series was created by preparing serial dilutions of activated recombinant MMP-9; produced as previously described (59). To measure elastinolytic activity, 15 µl of DQ elastin (DQ™-elastin, Thermo Fisher Scientific) [final concentration of 15 µg/mL] in Tris-HCl buffer (0.1 M, pH 8.0) was added to 5 µL BAL supernatant. A standard series was created by elastase dilutions (elastase from pig pancreas, Thermo Fisher scientific). Fluorescence was measured over time with the CLARIOstar microplate reader (BMG Labtech) for 1 h at 37°C. Metalloproteinase activity and serine protease activity were inhibited by the addition of EDTA (125 mM) or 4-(2-aminoethyl)-benzene-sulfonyl fluoride (AEBSF, 1 mg/mL, Pefabloc SC, Merck), respectively. The slopes of the kinetic curves were determined, and all data shown are represented as the equivalent of standard enzymatic activity.

Statistics

No normal distribution of data was detected as evaluated by the Shapiro-Wilk test. Mann-Whitney tests were used to statistically compare COVID-19 (n = 17) and influenza (n = 14) patient characteristics. A linear mixed model was used to detect statistical differences within and between COVID-19 (n = 31) and influenza (n = 14) BAL and blood samples. Correction for multiple samples per patient was done using a random intercept model. Statistical tests for comparison were two-sided, and $P< 0.05$ was considered significant. For data values below the lower detection limit, half the value of the lower detection limit was used for statistical comparison. The central lines in the boxes of the box-and-whisker plots represent the median, while the bounds of the boxes

represent the interquartile range, with the whiskers indicating the full distribution of the data. All outliers were included in the data and all data points are shown. Correlation analysis was performed calculating a repeated measures correlation coefficient with the rmcorr function in R and plotted utilizing a simple linear regression line. Statistical analysis was performed using RStudio version 1.4 and GraphPad Prism 9 (GraphPad Software, La Jolla, CA, USA) was employed for visualization of the data.

Study approval

Written informed consent was obtained from all study participants or their legal representatives according to the ethical guidelines of the Declaration of Helsinki. The Ethics Committee of the University Hospitals Leuven approved this study (S63881).

AUTHOR CONTRIBUTIONS

SC, MM, DS, PM, GO, JW, JV and PP designed the experiments. SC, MM, ACdC, CJ, LV, BM, MG, JV and PP developed methodology for the experiments & data analysis. SC, MM, ACdC, AN, CJ, LV, BM, EH and JW performed experiments and analyzed data. CJ, LV, PMe, GH, EW, AW and JW were involved in clinical data and patient sample collection. SC, MM, AN, CJ and BM visualized the data. MG, KM, PM, GO, REM, JW and PP acquired funding for this study. DS, PM, GO, REM, JW, JV and PP supervised this study. SC wrote the original draft of this manuscript and all authors reviewed, edited and approved the final version of the manuscript.

ACKNOWLEDGMENTS

We particularly thank Sandra Claes, Daisy Ceusters and Robin Hermans [Laboratory of Virology and Chemotherapy, Rega Institute, KU Leuven] for excellent technical assistance in the BSL3 facility and prof. Thomas Neyens [Leuven Biostatistics and Statistical Bioinformatics Centre (L-BioStat), KU Leuven] for providing advice on the statistical analysis of the data. This research was funded by a joint research grant to REM and PP from FWO-Vlaanderen and FAPESP (Grant No. G0F7519N-18/10990-1), a KU Leuven C1 Grant (C16/17/010) to PM, GO and PP and KU Leuven/UZ Leuven KOOR Grants for COVID-19 research (ESACOVID2-O2010) to JW and PP and to MG, KM, GO and PP. SC received a PhD fellowship from FWO-Vlaanderen. MM obtained a PhD fellowship supported by the L'Oréal – UNESCO for Women in Science Initiative and the FWO-Vlaanderen. ACdC is supported by a FAPESP PhD fellowship. JW and JV received postdoctoral fellowships from FWO-Vlaanderen. See Supplemental Acknowledgments for consortium details. The graphical abstract of this article was created with BioRender software.

REFERENCES

1. Wu Z, McGoogan JM. Characteristics of and Important Lessons From the Coronavirus Disease 2019 (COVID-19) Outbreak in China: Summary of a Report of 72 314 Cases From the Chinese Center for Disease Control and Prevention. *JAMA.* 2020;323(13):1239-42.
2. Moore JB, June CH. Cytokine release syndrome in severe COVID-19. *Science.* 2020;368(6490):473-4.
3. Qin C, et al. Dysregulation of Immune Response in Patients With Coronavirus 2019 (COVID-19) in Wuhan, China. *Clin Infect Dis.* 2020;71(15):762-8.
4. Liu J, et al. Neutrophil-to-lymphocyte ratio predicts critical illness patients with 2019 coronavirus disease in the early stage. *J Transl Med.* 2020;18(1):206.
5. Hidalgo A, et al. The Neutrophil Life Cycle. *Trends Immunol.* 2019;40(7):584-97.
6. Liew PX, Kubes P. The Neutrophil's Role During Health and Disease. *Physiol Rev.* 2019;99(2):1223-48.
7. Metzemaekers M, et al. Kinetics of peripheral blood neutrophils in severe coronavirus disease 2019. *Clin Transl Immunology.* 2021;10(4):e1271.
8. Schulte-Schrepping J, et al. Severe COVID-19 Is Marked by a Dysregulated Myeloid Cell Compartment. *Cell.* 2020;182(6):1419-40.e23.
9. Silvin A, et al. Elevated Calprotectin and Abnormal Myeloid Cell Subsets Discriminate Severe from Mild COVID-19. *Cell.* 2020;182(6):1401-18.e18.
10. Aschenbrenner AC, et al. Disease severity-specific neutrophil signatures in blood transcriptomes stratify COVID-19 patients. *Genome Med.* 2021;13(1):7.
11. Vanderbeke L, et al. Monocyte-driven atypical cytokine storm and aberrant neutrophil activation as key mediators of COVID-19 disease severity. *Nat Commun.* 2021;12(1):4117.

12. Veras FP, et al. SARS-CoV-2-triggered neutrophil extracellular traps mediate COVID-19 pathology. *J Exp Med.* 2020;217(12):e20201129.
13. Middleton EA, et al. Neutrophil extracellular traps contribute to immunothrombosis in COVID-19 acute respiratory distress syndrome. *Blood.* 2020;136(10):1169-79.
14. Sacchi A, et al. Early expansion of myeloid-derived suppressor cells inhibits SARS-CoV-2 specific T-cell response and may predict fatal COVID-19 outcome. *Cell Death Dis.* 2020;11(10):921.
15. Bost P, et al. Deciphering the state of immune silence in fatal COVID-19 patients. *Nat Commun.* 2021;12(1):1428.
16. Liao M, et al. Single-cell landscape of bronchoalveolar immune cells in patients with COVID-19. *Nat Med.* 2020;26(6):842-4.
17. Wauters E, et al. Discriminating mild from critical COVID-19 by innate and adaptive immune single-cell profiling of bronchoalveolar lavages. *Cell Res.* 2021;31(3):272-90.
18. Pandolfi L, et al. Broncho-alveolar inflammation in COVID-19 patients: a correlation with clinical outcome. *BMC Pulm Med.* 2020;20(1):301.
19. Rouzé A, et al. Relationship between SARS-CoV-2 infection and the incidence of ventilator-associated lower respiratory tract infections: a European multicenter cohort study. *Intensive Care Med.* 2021;47(2):188-98.
20. Buehler PK, et al. Bacterial pulmonary superinfections are associated with longer duration of ventilation in critically ill COVID-19 patients. *Cell Rep Med.* 2021;2(4):100229.
21. Prattes J, et al. Risk factors and outcome of pulmonary aspergillosis in critically ill coronavirus disease 2019 patients-a multinational observational study by the European

Confederation of Medical Mycology [published online Augustus 26, 2021]. *Clin Microbiol Infect.* https://doi.org/10.1016/j.cmi.2021.08.014.

22. Kadioglu A, et al. The integrins Mac-1 and alpha4beta1 perform crucial roles in neutrophil and T cell recruitment to lungs during Streptococcus pneumoniae infection. *J Immunol.* 2011;186(10):5907-15.

23. Casanova-Acebes M, et al. Rhythmic modulation of the hematopoietic niche through neutrophil clearance. *Cell.* 2013;153(5):1025-35.

24. Sengeløv H, et al. Mobilization of granules and secretory vesicles during in vivo exudation of human neutrophils. *J Immunol.* 1995;154(8):4157-65.

25. Metzemaekers M, et al. Neutrophil chemoattractant receptors in health and disease: double-edged swords. *Cell Mol Immunol.* 2020;17(5):433-50.

26. Zhang D, et al. Neutrophil ageing is regulated by the microbiome. *Nature.* 2015;525(7570):528-32.

27. Heinz A. Elastases and elastokines: elastin degradation and its significance in health and disease. *Crit Rev Biochem Mol Biol.* 2020;55(3):252-73.

28. Li S, et al. Clinical and pathological investigation of patients with severe COVID-19. *JCI Insight.* 2020;5(12):e138070.

29. Huang W, et al. The Inflammatory Factors Associated with Disease Severity to Predict COVID-19 Progression. *J Immunol.* 2021;206(7):1597-608.

30. Nossent EJ, et al. Pulmonary Procoagulant and Innate Immune Responses in Critically Ill COVID-19 Patients. *Front Immunol.* 2021;12:664209.

31. Reynolds D, et al. Comprehensive Immunologic Evaluation of Bronchoalveolar Lavage Samples from Human Patients with Moderate and Severe Seasonal Influenza and Severe COVID-19. *J Immunol.* 2021;207(5):1229-38.
32. Chua RL, et al. COVID-19 severity correlates with airway epithelium-immune cell interactions identified by single-cell analysis. *Nat Biotechnol.* 2020;38(8):970-9.
33. Xu G, et al. The differential immune responses to COVID-19 in peripheral and lung revealed by single-cell RNA sequencing. *Cell Discov.* 2020;6:73.
34. Van Damme J, et al. A novel, NH2-terminal sequence-characterized human monokine possessing neutrophil chemotactic, skin-reactive, and granulocytosis-promoting activity. *J Exp Med.* 1988;167(4):1364-76.
35. Zhao Y, et al. Clonal expansion and activation of tissue-resident memory-like Th17 cells expressing GM-CSF in the lungs of severe COVID-19 patients. *Sci Immunol.* 2021;6(56):eabf6692.
36. Pelletier M, et al. Evidence for a cross-talk between human neutrophils and Th17 cells. *Blood.* 2010;115(2):335-43.
37. Parackova Z, et al. Neutrophils mediate Th17 promotion in COVID-19 patients. *J Leukoc Biol.* 2021;109(1):73-6.
38. Radermecker C, et al. Neutrophil extracellular traps infiltrate the lung airway, interstitial, and vascular compartments in severe COVID-19. *J Exp Med.* 2020;217(12):e20201012.
39. Kaiser R, et al. Self-sustaining IL-8 loops drive a prothrombotic neutrophil phenotype in severe COVID-19. *JCI Insight.* 2021;6(18):e150862.

40. Fanger NA, et al. Activation of human T cells by major histocompatability complex class II expressing neutrophils: proliferation in the presence of superantigen, but not tetanus toxoid. *Blood.* 1997;89(11):4128-35.
41. Potey PM, et al. Neutrophils in the initiation and resolution of acute pulmonary inflammation: understanding biological function and therapeutic potential. *J Pathol.* 2019;247(5):672-85.
42. Cardinal-Fernández P, et al. Acute Respiratory Distress Syndrome and Diffuse Alveolar Damage. New Insights on a Complex Relationship. *Ann Am Thorac Soc.* 2017;14(6):844-50.
43. Wichmann D, et al. Autopsy Findings and Venous Thromboembolism in Patients With COVID-19. *Ann Intern Med.* 2020; 173(12):1030.
44. Zerimech F, et al. Protease-antiprotease imbalance in patients with severe COVID-19. *Clin Chem Lab Med.* 2021; 59(8):e330-e334.
45. Houghton AM. Matrix metalloproteinases in destructive lung disease. *Matrix Biol.* 2015;44-46:167-74.
46. Seren S, et al. Proteinase release from activated neutrophils in mechanically ventilated patients with non-COVID-19 and COVID-19 pneumonia. *Eur Respir J.* 2021;57(4): 2003755.
47. Williams SE, et al. SLPI and elafin: one glove, many fingers. *Clin Sci (Lond).* 2006;110(1):21-35.
48. Vandooren J, et al. Neutrophils and Activated Macrophages Control Mucosal Immunity by Proteolytic Cleavage of Antileukoproteinase. *Front Immunol.* 2018;9:1154.

49. Thierry AR. Anti-protease Treatments Targeting Plasmin(ogen) and Neutrophil Elastase May Be Beneficial in Fighting COVID-19. *Physiol Rev.* 2020;100(4):1597-8.

50. Wettstein L, et al. Alpha-1 antitrypsin inhibits TMPRSS2 protease activity and SARS-CoV-2 infection. *Nat Commun.* 2021;12(1):1726.

51. Yang C, et al. Alpha-1 Antitrypsin for COVID-19 Treatment: Dual Role in Antiviral Infection and Anti-Inflammation. *Front Pharmacol.* 2020;11:615398.

52. de Loyola MB, et al. Alpha-1-antitrypsin: A possible host protective factor against Covid-19. *Rev Med Virol.* 2021;31(2):e2157.

53. Bai X, et al. Hypothesis: Alpha-1-antitrypsin is a promising treatment option for COVID-19. *Med Hypotheses.* 2021;146:110394.

54. Chalmers JD, et al. Phase 2 Trial of the DPP-1 Inhibitor Brensocatib in Bronchiectasis. *N Engl J Med.* 2020;383(22):2127-37.

55. Root-Bernstein R. Innate Receptor Activation Patterns Involving TLR and NLR Synergisms in COVID-19, ALI/ARDS and Sepsis Cytokine Storms: A Review and Model Making Novel Predictions and Therapeutic Suggestions. *Int J Mol Sci.* 2021;22(4): 2108.

56. Galani IE, et al. Untuned antiviral immunity in COVID-19 revealed by temporal type I/III interferon patterns and flu comparison. *Nat Immunol.* 2021;22(1):32-40.

57. Zhang Q, et al. Inborn errors of type I IFN immunity in patients with life-threatening COVID-19. *Science.* 2020;370(6515):eabd4570.

58. Koehler P, et al. Defining and managing COVID-19-associated pulmonary aspergillosis: the 2020 ECMM/ISHAM consensus criteria for research and clinical guidance. *Lancet Infect Dis.* 2021;21(6):e149-e62.

687 59. Van den Steen PE, et al. The hemopexin and O-glycosylated domains tune gelatinase
688 B/MMP-9 bioavailability via inhibition and binding to cargo receptors. *J Biol Chem.*
689 2006;281(27):18626-37.

690 **FIGURES**

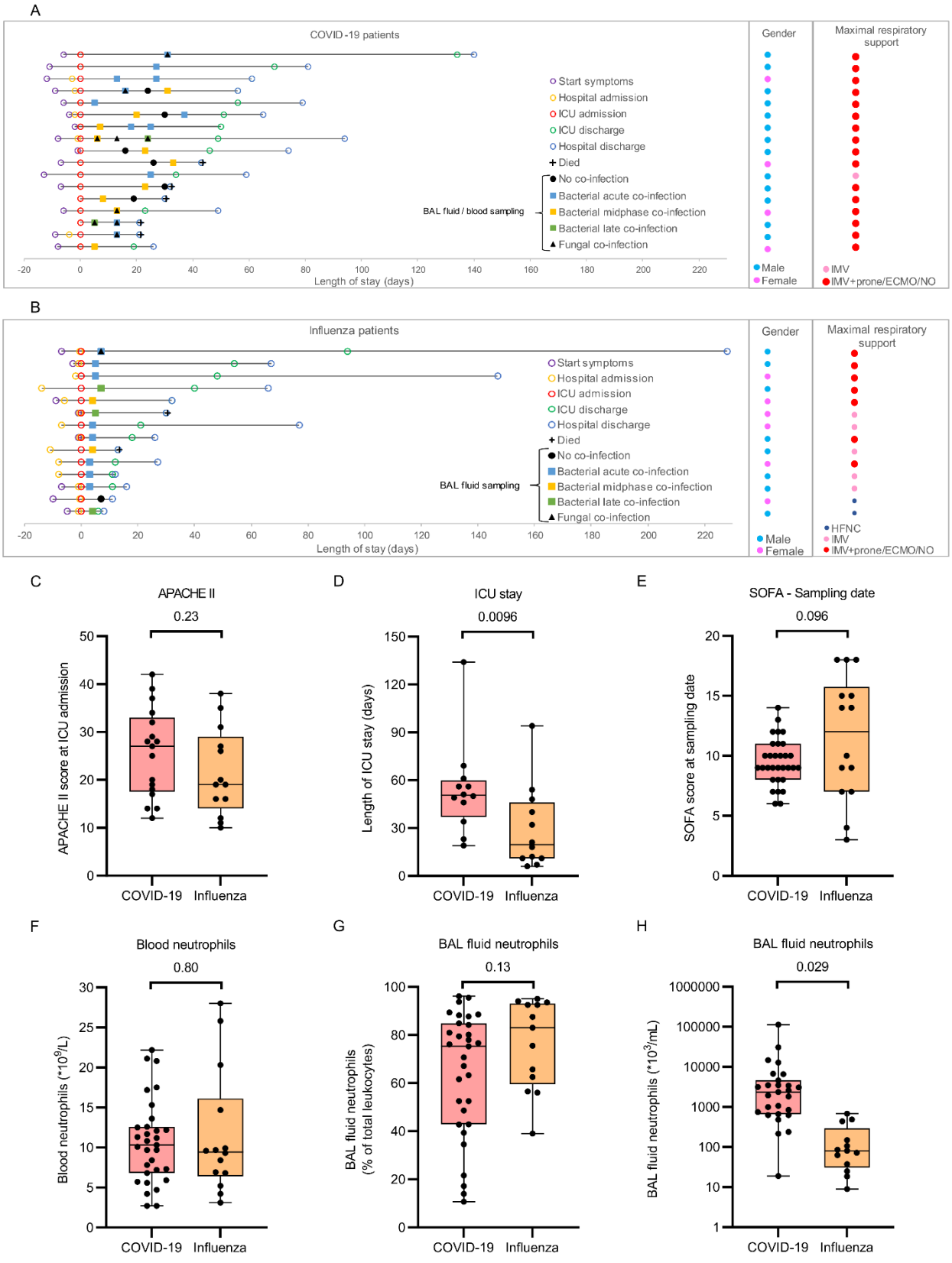
A
COVID-19 patients
Start symptoms
Hospital admission
ICU admission
ICU discharge
Hospital discharge
Died
BAL fluid / blood sampling
No co-infection
Bacterial acute co-infection
Bacterial midphase co-infection
Bacterial late co-infection
Fungal co-infection
Length of stay (days)
Gender
Male
Female
Maximal respiratory support
IMV
IMV+prone/ECMO/NO
B
Influenza patients
BAL fluid sampling
HFNC
C
APACHE II
0.23
APACHE II score at ICU admission
D
ICU stay
0.0096
Length of ICU stay (days)
E
SOFA - Sampling date
0.096
SOFA score at sampling date
F
Blood neutrophils
0.80
Blood neutrophils (*10^9/L)
G
BAL fluid neutrophils
0.13
BAL fluid neutrophils (% of total leukocytes)
H
BAL fluid neutrophils
0.029
BAL fluid neutrophils (*10^3/mL)
COVID-19
Influenza

Figure 1. **COVID-19 and influenza patient characteristics. (A-B)** Clinical course timeline of the **(A)** COVID-19 (*n* = 17) and **(B)** influenza (*n* = 14) ICU patients. Patients are ranked based on the length of ICU stay with time point 0 representing ICU admission. The co-infection status at the moment of BAL/blood sampling, is indicated. Samples were categorized based on the absence of a co-infection or the acute phase (clinical/biochemical worsening and antibiotics not yet or recently started), midphase (signs of improvement with ongoing antibiotic therapy) or late phase (final days of antibiotic therapy nearing complete remission) of a bacterial co-infection based on the timing of the BAL sample analyzed relative to the co-infection time course. A fungal co-infection was diagnosed based on radiological abnormalities in combination with clinical signs and mycological evidence (positive galactomannan in BAL and/or serum and/or presence of *Aspergillus fumigatus* in BAL culture). Next to the timeline, gender and maximal respiratory support during hospital stay are shown. **(C)** Acute Physiology And Chronic Health Evaluation II (APACHE II) score at ICU admission and **(D)** length of ICU stay of all patients included in the study (patients who died are excluded). **(E)** Sequential Organ Failure Assessment (SOFA) score at the moment BAL fluid and blood samples were collected from COVID-19 (*n* = 31) and influenza patients (*n* = 14). **(F-H)** Blood and BAL fluid neutrophil counts within the samples collected. Data are shown as box-and-whisker plots (box: median with interquartile range, whiskers: full data distribution) with each dot representing an individual patient (sample) and statistically analyzed by a Mann-Whitney test or a linear mixed model with correction for multiple samples per patient using a random intercept model, where appropriate. ECMO, extracorporeal membrane oxygenation; HFNC, high flow nasal cannula; IMV, invasive mechanical ventilation.

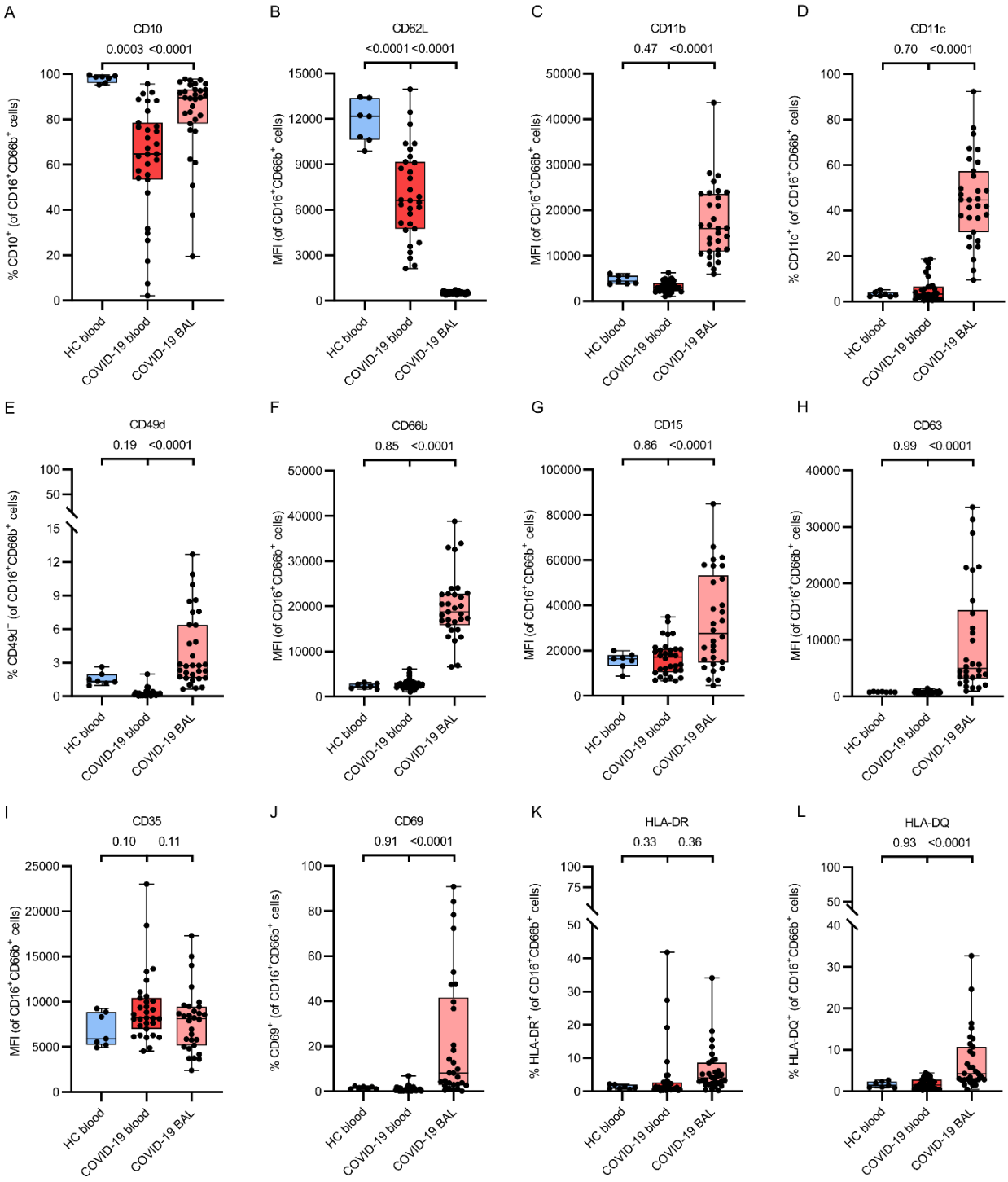
A
CD10
0.0003 <0.0001
% CD10+ (of CD16+CD66b+ cells)
B
CD62L
<0.0001 <0.0001
MFI (of CD16+CD66b+ cells)
C
CD11b
0.47 <0.0001
MFI (of CD16+CD66b+ cells)
D
CD11c
0.70 <0.0001
% CD11c+ (of CD16+CD66b+ cells)
E
CD49d
0.19 <0.0001
% CD49d+ (of CD16+CD66b+ cells)
F
CD66b
0.85 <0.0001
MFI (of CD16+CD66b+ cells)
G
CD15
0.86 <0.0001
MFI (of CD16+CD66b+ cells)
H
CD63
0.99 <0.0001
MFI (of CD16+CD66b+ cells)
I
CD35
0.10 0.11
MFI (of CD16+CD66b+ cells)
J
CD69
0.91 <0.0001
% CD69+ (of CD16+CD66b+ cells)
K
HLA-DR
0.33 0.36
% HLA-DR+ (of CD16+CD66b+ cells)
L
HLA-DQ
0.93 <0.0001
% HLA-DQ+ (of CD16+CD66b+ cells)
HC blood
COVID-19 blood
COVID-19 BAL

712

Figure 2. **Phenotypical characterization of adhesion molecules and activation/maturation markers on BAL fluid and peripheral blood neutrophils from patients with severe COVID-19.** Flow cytometry was used to evaluate the surface expression of **(A)** CD10, **(B)** CD62L, **(C)** CD11b, (**D)** CD11c, **(E)** CD49d, **(F)** CD66b, **(G)** CD15, **(H)** CD63, **(I)** CD35, **(J)** CD69, **(K)** HLA-DR and **(L)** HLA-DQ on neutrophils (gated as $CD16^{+}CD66b^{+}$ cells) from paired blood and BAL fluid samples from COVID-19 patients (n = 31) and blood samples from healthy controls (HC) (n = 7). Results represent percentages of positive neutrophils or median fluorescence intensity (MFI). Data are shown as box-and-whisker plots (box: median with interquartile range, whiskers: full data distribution) with each dot representing an individual patient sample and statistically analyzed by a linear mixed model with correction for multiple samples per patient using a random intercept model.

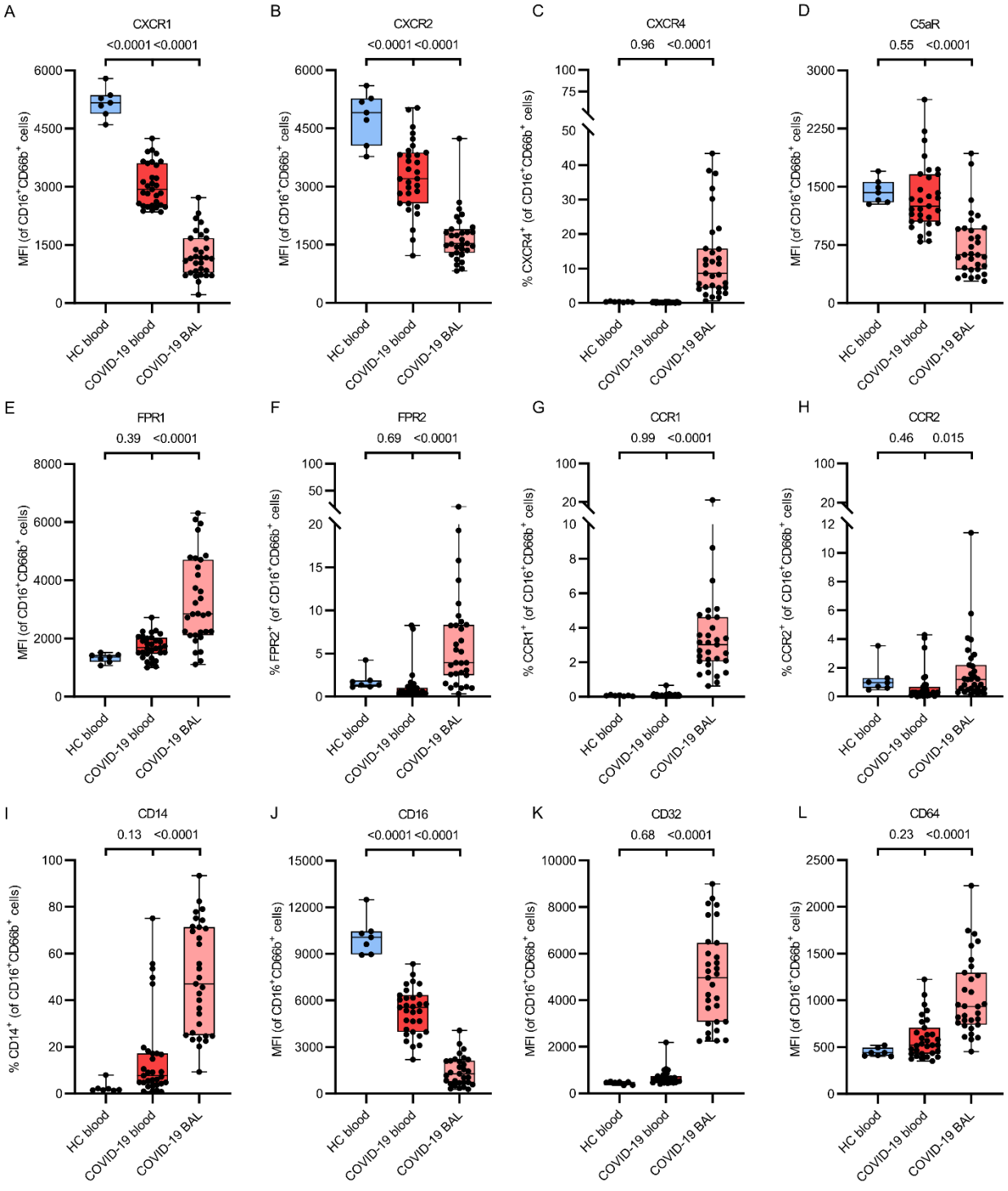
A
CXCR1
<0.0001 <0.0001
MFI (of CD16+CD66b+ cells)
B
CXCR2
<0.0001 <0.0001
MFI (of CD16+CD66b+ cells)
C
CXCR4
0.96 <0.0001
% CXCR4+ (of CD16+CD66b+ cells)
D
C5aR
0.55 <0.0001
MFI (of CD16+CD66b+ cells)
E
FPR1
0.39 <0.0001
MFI (of CD16+CD66b+ cells)
F
FPR2
0.69 <0.0001
% FPR2+ (of CD16+CD66b+ cells)
G
CCR1
0.99 <0.0001
% CCR1+ (of CD16+CD66b+ cells)
H
CCR2
0.46 0.015
% CCR2+ (of CD16+CD66b+ cells)
I
CD14
0.13 <0.0001
% CD14+ (of CD16+CD66b+ cells)
J
CD16
<0.0001 <0.0001
MFI (of CD16+CD66b+ cells)
K
CD32
0.68 <0.0001
MFI (of CD16+CD66b+ cells)
L
CD64
0.23 <0.0001
MFI (of CD16+CD66b+ cells)
HC blood
COVID-19 blood
COVID-19 BAL

724

Figure 3. **Phenotypical characterization of chemoattractant and Fcγ receptors on BAL fluid and peripheral blood neutrophils from patients with severe COVID-19.** Flow cytometry was used to evaluate the surface expression of **(A)** CXCR1, **(B)** CXCR2, **(C)** CXCR4, (**D)** C5aR, **(E)** FPR1, **(F)** FPR2, **(G)** CCR1, **(H)** CCR2, **(I)** CD14, **(J)** CD16, **(K)** CD32 and **(L)** CD64 on neutrophils (gated as $CD16^{+}CD66b^{+}$ cells) from paired blood and BAL fluid samples from COVID-19 patients (n = 31) and blood samples from healthy controls (HC) (n = 7). Results represent percentages of positive neutrophils or median fluorescence intensity (MFI). Data are shown as box-and-whisker plots (box: median with interquartile range, whiskers: full data distribution) with each dot representing an individual patient sample and statistically analyzed by a linear mixed model with correction for multiple samples per patient using a random intercept model.

736

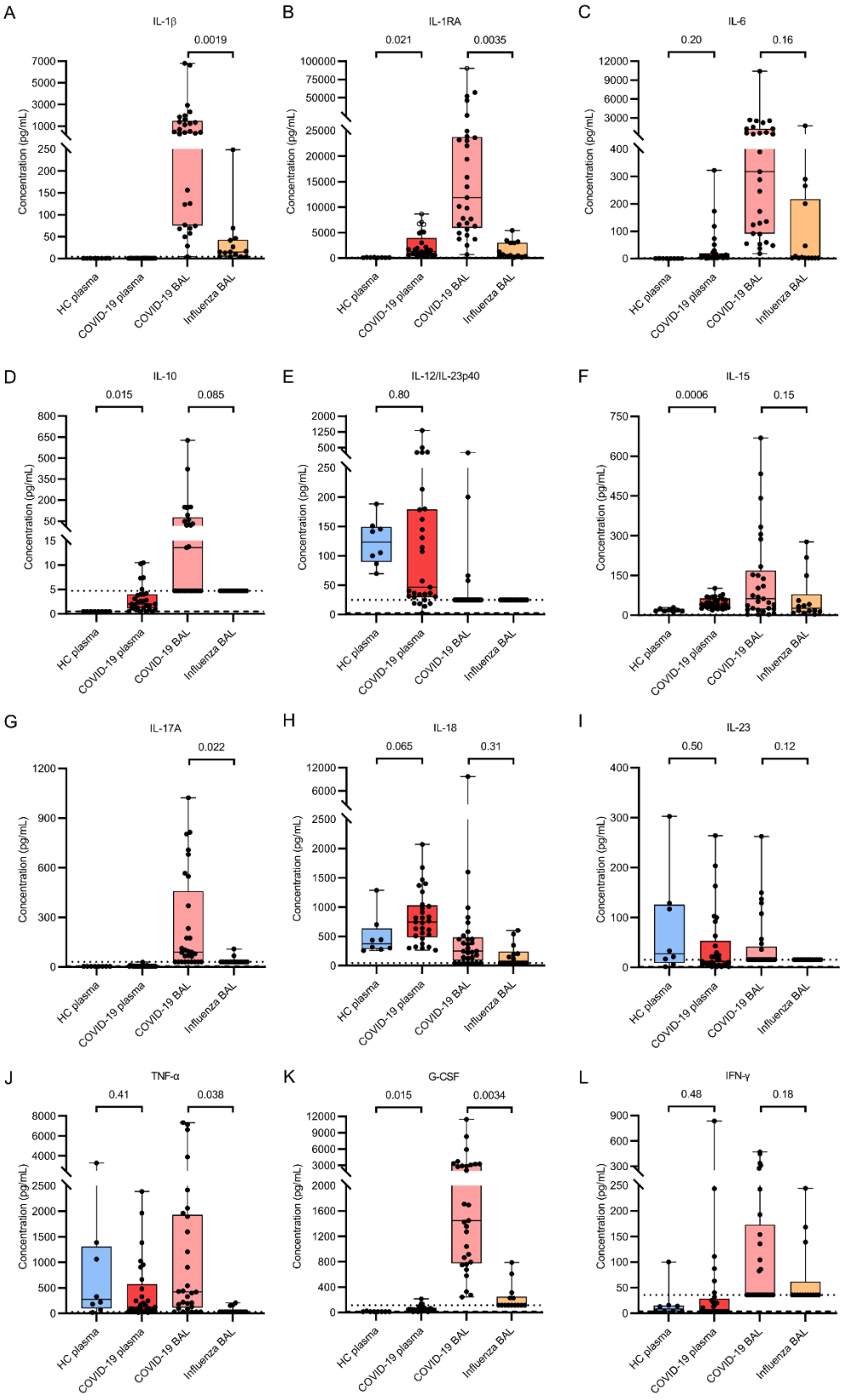
A
IL-1β
0.0019
B
IL-1RA
0.021
0.0035
C
IL-6
0.20
0.16
D
IL-10
0.015
0.085
E
IL-12/IL-23p40
0.80
F
IL-15
0.0006
0.15
G
IL-17A
0.022
H
IL-18
0.065
0.31
I
IL-23
0.50
0.12
J
TNF-α
0.41
0.038
K
G-CSF
0.015
0.0034
L
IFN-γ
0.48
0.18
Concentration (pg/mL)
HC plasma
COVID-19 plasma
COVID-19 BAL
Influenza BAL

Figure 4. **Quantification of cytokines in plasma and BAL fluid from patients with severe COVID-19 or influenza.** Multiplex technology was used to determine concentrations of **(A)** IL-1β, **(B)** IL-1RA, **(C)** IL-6, **(D)** IL-10, (**E)** IL-12/IL-23p40, **(F)** IL-15, **(G)** IL-17A, **(H)** IL-18, **(I)** IL-23, **(J)** TNF-α, **(K)** G-CSF and **(L)** IFN-γ in plasma and BAL fluid samples from COVID-19 patients (n = 29), plasma samples from healthy controls (HC) (n = 8) and BAL fluid samples from influenza patients (n = 14). Data are shown as box-and-whisker plots (box: median with interquartile range, whiskers: full data distribution) with each dot representing an individual patient sample. The dashed lines indicate the lower detection limits (BAL samples were diluted 1/10). Open symbols indicate values above the upper detection limit. Data were statistically analyzed by a linear mixed model with correction for multiple samples per patient using a random intercept model.

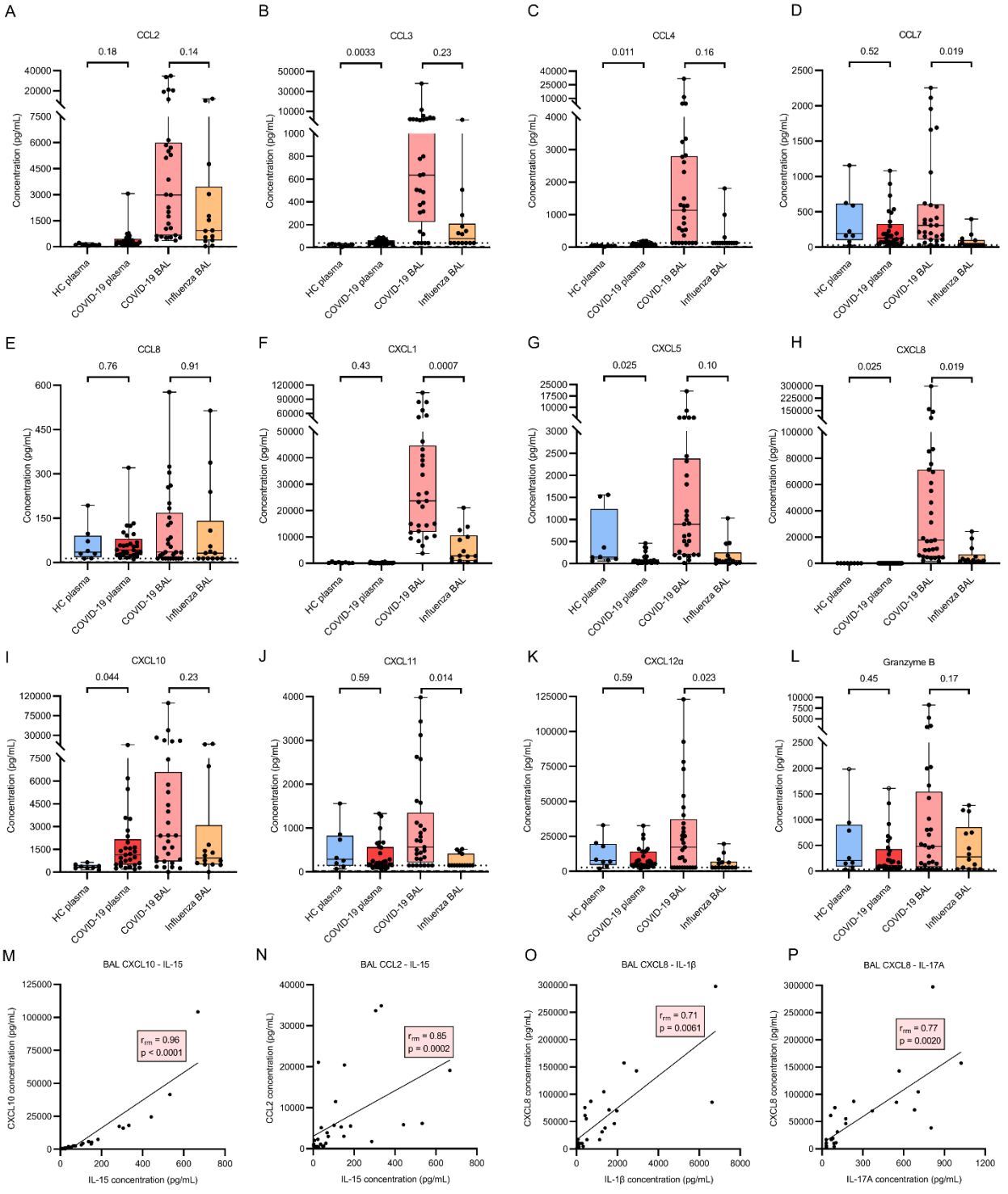
A
CCL2
0.18
0.14
B
CCL3
0.0033
0.23
C
CCL4
0.011
0.16
D
CCL7
0.52
0.019
E
CCL8
0.76
0.91
F
CXCL1
0.43
0.0007
G
CXCL5
0.025
0.10
H
CXCL8
0.025
0.019
I
CXCL10
0.044
0.23
J
CXCL11
0.59
0.014
K
CXCL12α
0.59
0.023
L
Granzyme B
0.45
0.17
Concentration (pg/mL)
HC plasma
COVID-19 plasma
COVID-19 BAL
Influenza BAL
M
BAL CXCL10 - IL-15
r_rm = 0.96
p < 0.0001
CXCL10 concentration (pg/mL)
IL-15 concentration (pg/mL)
N
BAL CCL2 - IL-15
r_rm = 0.85
p = 0.0002
CCL2 concentration (pg/mL)
IL-15 concentration (pg/mL)
O
BAL CXCL8 - IL-1β
r_rm = 0.71
p = 0.0061
CXCL8 concentration (pg/mL)
IL-1β concentration (pg/mL)
P
BAL CXCL8 - IL-17A
r_rm = 0.77
p = 0.0020
CXCL8 concentration (pg/mL)
IL-17A concentration (pg/mL)

748

Figure 5. **Quantification of biomarkers in plasma and BAL fluid from patients with severe COVID-19 or influenza.** Multiplex and ELISA technology was used to determine concentrations of **(A)** CCL2, **(B)** CCL3, **(C)** CCL4, **(D)** CCL7, (**E)** CCL8, **(F)** CXCL1, **(G)** CXCL5, **(H)** CXCL8, **(I)** CXCL10, **(J)** CXCL11, **(K)** CXCL12α and **(L)** granzyme B in plasma and BAL fluid samples from COVID-19 patients (*n* = 29), plasma samples from healthy controls (HC) (*n* = 8) and BAL fluid samples from influenza patients (*n* = 14). (**M-P)** Correlation between cytokine and chemokine levels measured in the BAL fluid of COVID-19 patients. Data are shown as box-and-whisker plots (box: median with interquartile range, whiskers: full data distribution) with each dot representing an individual patient sample. The dashed lines indicate the lower detection limits (BAL samples were diluted 1/10). Data were statistically analyzed by a linear mixed model with correction for multiple samples per patient using a random intercept model. Correlation analysis was performed calculating a repeated measures correlation coefficient and plotted utilizing a simple linear regression line.

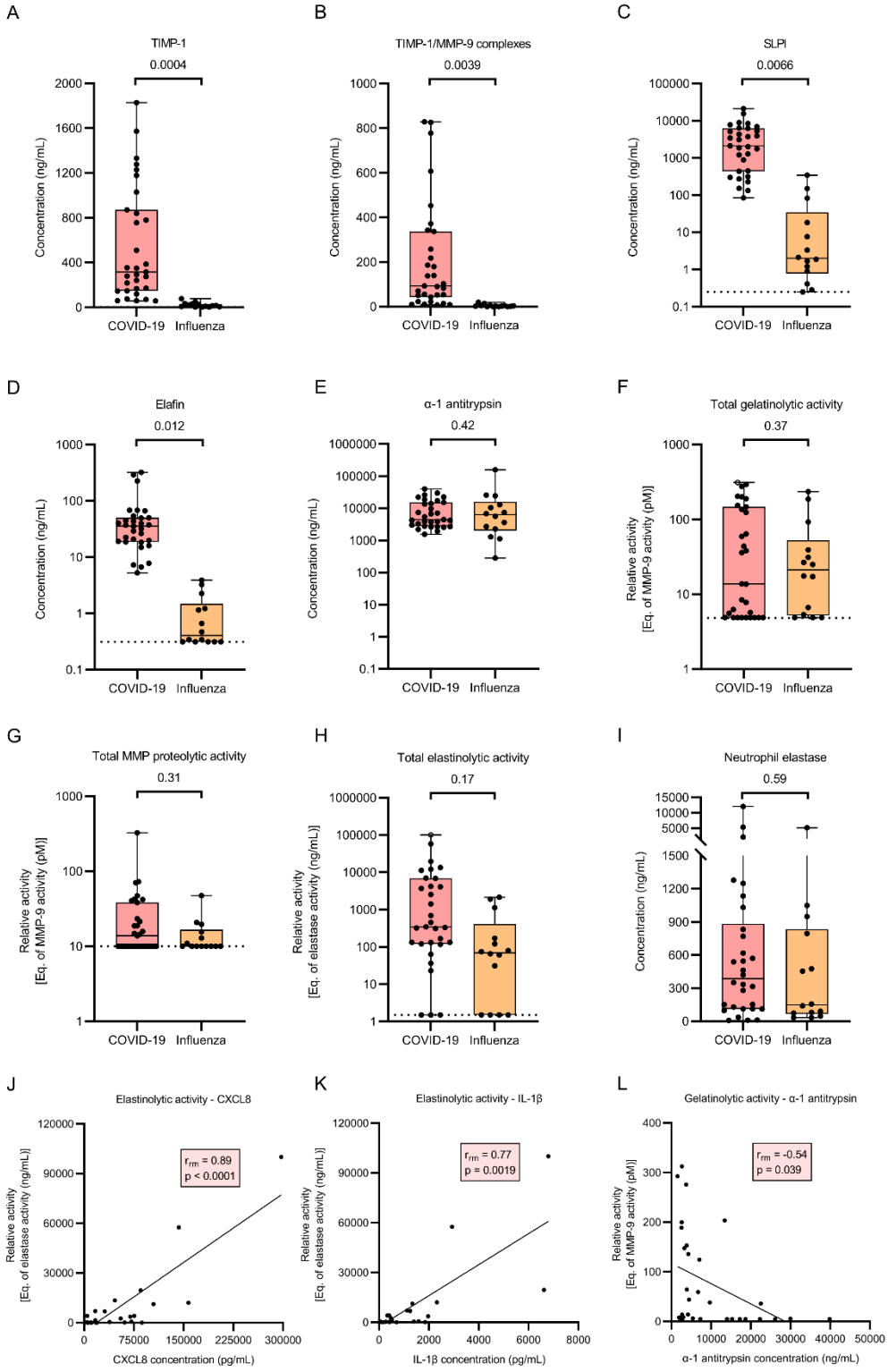
A
TIMP-1
0.0004
Concentration (ng/mL)
COVID-19
Influenza
B
TIMP-1/MMP-9 complexes
0.0039
C
SLPI
0.0066
D
Elafin
0.012
E
α-1 antitrypsin
0.42
F
Total gelatinolytic activity
0.37
Relative activity [Eq. of MMP-9 activity (pM)]
G
Total MMP proteolytic activity
0.31
H
Total elastinolytic activity
0.17
Relative activity [Eq. of elastase activity (ng/mL)]
I
Neutrophil elastase
0.59
J
Elastinolytic activity - CXCL8
r_{rm} = 0.89
p < 0.0001
CXCL8 concentration (pg/mL)
K
Elastinolytic activity - IL-1β
r_{rm} = 0.77
p = 0.0019
IL-1β concentration (pg/mL)
L
Gelatinolytic activity - α-1 antitrypsin
r_{rm} = -0.54
p = 0.039
α-1 antitrypsin concentration (ng/mL)

Figure 6. **Quantification of protease activity, protease and protease inhibitor levels in BAL fluid from patients with severe COVID-19 or influenza.** ELISA was used to determine concentrations of **(A)** TIMP-1, **(B)** TIMP-1/MMP-9 complexes, **(C)** SLPI, **(D)** elafin and **(E)** α-1 antitrypsin (serpin A1) in BAL fluid samples from COVID-19 patients (n = 31) and influenza patients (n = 14). **(F)** Total gelatinolytic activity, as determined in a kinetic assay measuring degradation of a fluorogenic gelatin substrate, **(G)** total MMP proteolytic activity, as determined measuring degradation of a fluorogenic omni MMP substrate, (**H)** total elastinolytic activity, as determined measuring degradation of a fluorogenic elastin substrate and **(I)** neutrophil elastase levels (quantified by ELISA) were measured within the BAL fluid samples. **(J-L)** Correlation between chemokine/cytokine levels, proteolytic activity and protease inhibitors measured in the BAL fluid of COVID-19 patients. Data are shown as box-and-whisker plots (box: median with interquartile range, whiskers: full data distribution) with each dot representing an individual patient sample. The dashed lines indicate the lower detection limits. Open symbols indicate values above the upper detection limit. Data were statistically analyzed by a linear mixed model with correction for multiple samples per patient using a random intercept model. Correlation analysis was performed calculating a repeated measures correlation coefficient and plotted utilizing a simple linear regression line.

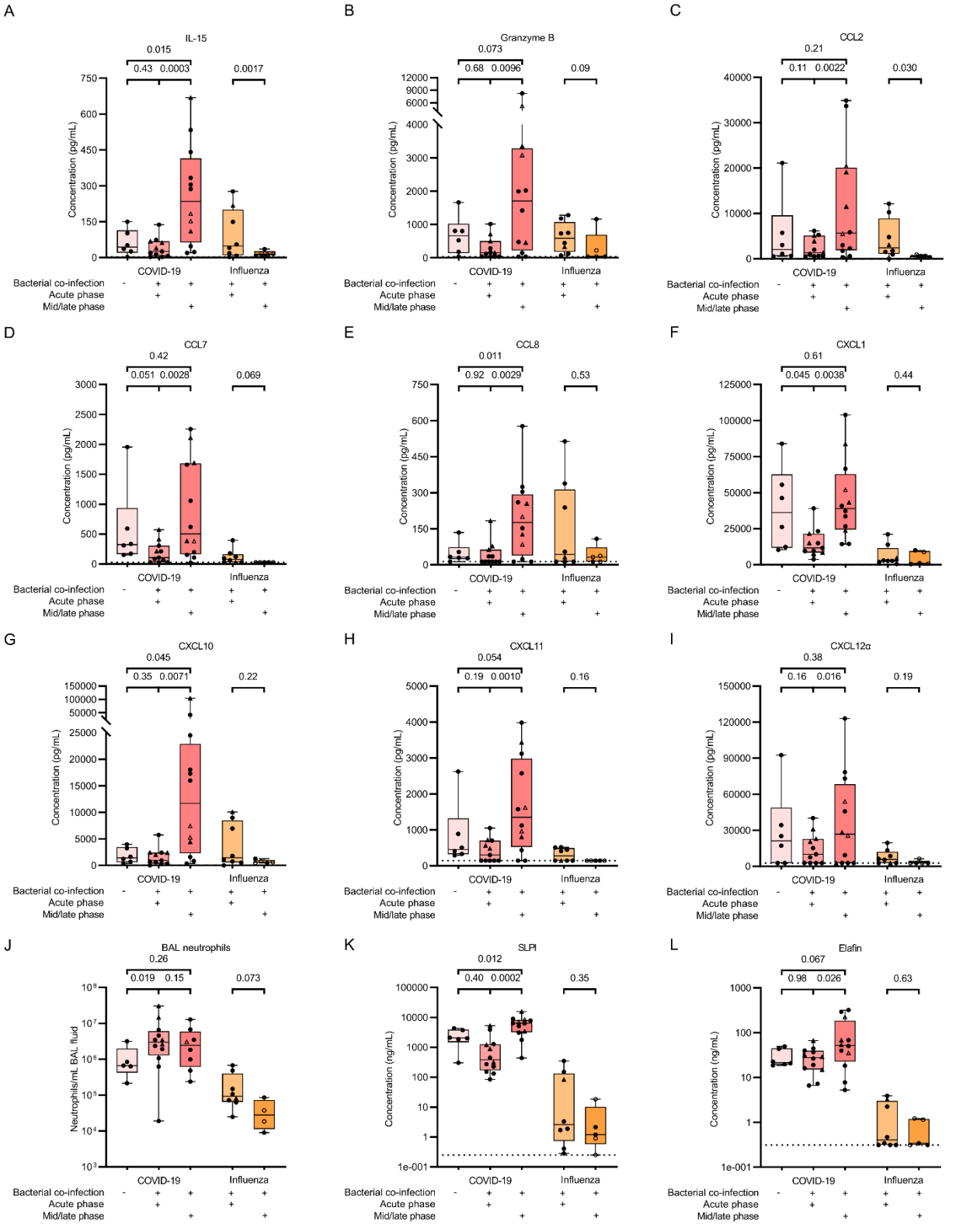
A
IL-15
0.015
0.43
0.0003
0.0017
Concentration (pg/mL)
750
600
450
300
150
0
COVID-19
Influenza
Bacterial co-infection - + + + +
Acute phase + + +
Mid/late phase + +
B
Granzyme B
0.073
0.68
0.0096
0.09
12000
9000
6000
4000
3000
2000
1000
0
C
CCL2
0.21
0.11
0.0022
0.030
40000
30000
20000
10000
0
D
CCL7
0.42
0.051
0.0028
0.069
3000
2500
2000
1500
1000
500
0
E
CCL8
0.011
0.92
0.0029
0.53
F
CXCL1
0.61
0.045
0.0038
0.44
125000
100000
75000
50000
25000
G
CXCL10
0.045
0.35
0.0071
0.22
150000
100000
50000
25000
20000
15000
10000
5000
H
CXCL11
0.054
0.19
0.0010
0.16
I
CXCL12α
0.38
0.16
0.016
0.19
120000
90000
60000
30000
J
BAL neutrophils
0.26
0.019
0.15
0.073
Neutrophils/mL BAL fluid
10^8
10^7
10^6
10^5
10^4
10^3
K
SLPI
0.012
0.40
0.0002
0.35
Concentration (ng/mL)
100000
10000
1000
100
10
1
1e-001
L
Elafin
0.067
0.98
0.026
0.63

780

Figure 7. **Quantification of biomarkers in BAL fluid from patients with severe COVID-19 or influenza, stratified by the timing of a bacterial co-infection.** Multiplex and ELISA technology was used to determine concentrations of **(A)** IL-15, **(B)** granzyme B, **(C)** CCL2, **(D)** CCL7, (**E)** CCL8, **(F)** CXCL1, **(G)** CXCL10, **(H)** CXCL11 and **(I)** CXCL12α in COVID-19 and influenza BAL fluid samples. **(J)** BAL fluid neutrophil counts. **(K-L)** ELISA was used to determine **(K)** SLPI and **(L)** elafin concentrations in the BAL fluids. All COVID-19 samples were categorized based on the absence of a co-infection (n = 6) or the acute phase (n = 11) or mid/late phase of a bacterial co-infection (n = 12) based on the timing of the BAL sampling relative to the co-infection time course. Influenza patient samples were also categorized in the acute phase (n = 8) and the mid/late phase (n = 5) of a bacterial co-infection. Data are shown as box-and-whisker plots (box: median with interquartile range, whiskers: full data distribution) with each dot representing an individual patient sample. The dashed lines indicate the lower detection limits. In the mid/late groups, open symbols indicate samples taken during the late phase of the bacterial co-infection, the others are taken during the midphase of the bacterial co-infection. Triangles indicate samples with an additional fungal co-infection. Data were statistically analyzed by a linear mixed model with correction for multiple samples per patient using a random intercept model or a Mann-Whitney test, where appropriate.

TABLES

		COVID-19 patients (*n* = 17)	Influenza patients (*n* = 14)	P-value
Age (years)		68 (54-76)	58 (42-71)	0.18
Sex	Male	13/17 (76 %)	8/14 (57 %)	0.44
	Female	4/17 (24 %)	6/14 (43 %)	
BMI (kg/m²)		31 (25-39)	29 (22-32)	0.14
Co-morbidities	Diabetes	5/17 (29 %)	0/14 (0 %)	0.048
	Cardiovascular disease	12/17 (71 %)	5/14 (36 %)	0.076
	Chronic pulmonary disease	4/17 (24 %)	3/14 (21 %)	0.99
	Rheumatologic disease	3/17 (18 %)	4/14 (29 %)	0.67
	Renal disease	1/17 (6 %)	1/14 (7 %)	0.99
	Malignancy	3/17 (18 %)	2/14 (14 %)	0.99
Time from onset of symptoms to ICU admission (days)		7 (6-9)	6 (2-9)	0.28
Time between hospital and ICU admission (days)		0 (0-2)	2 (0-8)	0.011
APACHE II score at ICU admission		27 (18-33)	19 (14-29)	0.23
Length of ICU stay (days)[$]		51 (37-60)	20 (11-46)	0.0096
Length of total hospital stay (days)[$]		67 (58-81)	33 (18-83)	0.27
Mortality		5/17 (29 %)	2/14 (14 %)	0.41

		COVID-19 patient samples (n = 31)	Influenza patient samples (n = 14)	
SOFA score at moment of sampling		9 (8-11)	12 (7-16)	0.096
Respiratory support at time of sampling	HFNC	0/31 (0 %)	2/14 (14 %)	0.092
	IMV	31/31 (100 %)	12/14 (86 %)	0.092
	Proning	6/31 (19 %)	2/14 (14 %)	0.99
	ECMO	13/31 (42 %)	4/14 (29 %)	0.51
	Inhaled NO	7/31 (23 %)	2/14 (14 %)	0.70
Blood	Leukocyte count (*10^9/L)	12 (8-16)	12 (8-20)	0.58
	Neutrophil count (*10^9/L)	10 (7-13)	10 (6-16)	0.80
	Eosinophil count (*10^9/L)	0 (0-0.4)	0 (0-0.1)	0.098
	Lymphocyte count (*10^9/L)	0.6 (0.4-0.8)	0.6 (0.3-1.2)	0.52
	Monocyte count (*10^9/L)	0.5 (0.4-0.8)	0.5 (0.3-0.8)	0.89
	D-dimer (µg/L)	2038 (1010-6135)	ND	/
	CRP (mg/L)	68 (21-144)	113 (66-249)	0.11
BAL fluid	Leukocyte count (*10^3/mL)	3040 (1550-5840)	95 (37-234)	0.019
	Neutrophil (% of total leukocytes)	75 (43-85)	83 (60-93)	0.13
	Eosinophil (% of total leukocytes)	ND	0 (0-0.5)	/

	Lymphocyte (% of total leukocytes)	ND	2.5 (0.5-3.8)	/
	Macrophage (% of total leukocytes)	ND	14 (7-38)	/
Treatment <24 h of sampling	Antibiotic treatment[#]	22/31 (71 %)	12/14 (86 %)	0.46
	Antifungal treatment[#]	8/31 (26 %)	8/14 (57 %)	0.053
	Antiviral treatment[#]	0/31 (0 %)	14/14 (100 %)	<0.0001
	Corticosteroids	25/31 (81 %)	9/14 (64 %)	0.28
	Heparin	31/31 (100 %)	14/14 (100 %)	0.99

802

Table 1. COVID-19 and influenza patient characteristics. General characteristics of patients included in the study (17 COVID-19 and 14 influenza patients) are indicated in the first part of the table. The lower part of the table contains information about the blood and BAL samples collected from these patients (31 parallel blood and BAL samples from COVID-19 patients and 14 BAL samples from influenza patients). Continuous variables are presented as median (interquartile range). Categorical variables are presented as counts (percentage). Data are statistically analyzed by a Mann-Whitney test or a linear mixed model with correction for multiple samples per patient using a random intercept model, where appropriate. Proportions are compared using a Fisher's exact test. $ Patients who died are excluded. # Antibiotic treatments: amoxicillin, piperacillin/tazobactam, clavulanic acid, cefepime, levofloxacin, vancomycin, ceftazidime, ceftriaxone, erythromycin or meropenem. Antifungal treatments: posaconazole or voriconazole. Antiviral treatment: oseltamivir. APACHE II, Acute Physiology And Chronic Health Evaluation II; BAL, broncho-alveolar lavage; CRP, C-reactive protein; ECMO: extracorporeal membrane oxygenation; HFNC, high flow nasal cannula; ICU, intensive care unit; IMV, invasive mechanical ventilation; ND, not determined; SOFA, Sequential Organ Failure Assessment.